The Di-Iron Subsite of All-Iron Hydrogenase: Mechanism of Cyanation of a Synthetic {2Fe3S} – Carbonyl Assembly

Simon J. George, Zhen Cui, Mathieu Razavet, and Christopher J. Pickett*[a]

Abstract: This paper describes the kinetics and intimate mechanisms associated with cyanation of {2Fe3S} assemblies to give species structurally related to the subsite of all-iron hydrogenase. Stopped-flow FTIR spectroscopy has enabled the quantitation of the dynamics of five well-defined steps that experimentally illustrate the role of bridging carbonyls in the assembly of the dicyanide species, how on – off sulfur ligation can have a dramatic effect on cyanation kinetics and how the {2Fe3S} core stabilises bridging carbonyl species.

Keywords: bioinorganic chemistry · bridging ligands · carbonyl ligands · hydrogenases · metal – metal interactions · stopped-flow IR spectroscopy

Introduction

X-ray crystallographic data for Fe-only hydrogenases isolated from *Desulfovibrio desulfuricans*[1] and *Clostridium pasteurianum*[1][2] together with infrared evidence show that the active centre of the enzyme possesses a {2Fe3S} subsite in which a terminal CO, a bridging CO and a CN ligand are bound at each iron centre.[3] The two Fe atoms of the subsite share two bridging sulfur ligands of a 1,3-propanedithiolate or related azapropanedithiolate unit[4] with one of the Fe atoms additionally sulfur-ligated by a cysteinyl ligand bridged to a {4Fe4S} cluster (Figure 1a). This cluster/subsite assembly is termed the H cluster. Together, the protein structural data and FTIR studies of the enzyme have stimulated much effort directed towards the synthesis of free-standing structures related to the subsite of the H cluster. This has been both to provide insight into structure/spectroscopy/function of the natural system and to uncover new electrocatalysts for hydrogen evolution/uptake pertinent to energy transduction.[5–10]

Molecules with a {2Fe2S}-propanedithiolate[5] or with a azapropanedithiolate core[6] have been synthesised, and they possess *some* of the structural elements of the CO-inhibited subsite. However, they lack differential 2S/3S ligation of the iron sites as well as a CO bridging group. Recently, we have shown that formal backbone modification of a propanedithiolate ligand allows access to the {2Fe3S} – carbonyl $[Fe_2(CO)_5\{MeSCH_2C(Me)(CH_2S)_2\}]$ **A** and also its benzyl thioether analogue. These molecules possess differential S ligation of the iron atoms, as occurs in the natural subsite (Figure 1a and b).[7] Importantly, **A** reacts with $[NEt_4][CN]$ to form a dicyanide with a bridging carbonyl group $[Fe_2(CO)_3(\mu\text{-}CO)\{MeSCH_2C(Me)(CH_2S)_2\}(CN)_2]^{2-}$ (**D**). This dianion possesses the key attributes of the natural subsite, namely a {2Fe3S} core with differentiated irons each ligated by cyanide and bridged by a carbonyl.[7] Compound **D** slowly rearranges at ambient temperature to the thermodynamically stable product $[Fe_2(CO)_4\{MeSCH_2C(Me)(CH_2S)_2\}(CN)_2]^{2-}$ (**E**), in

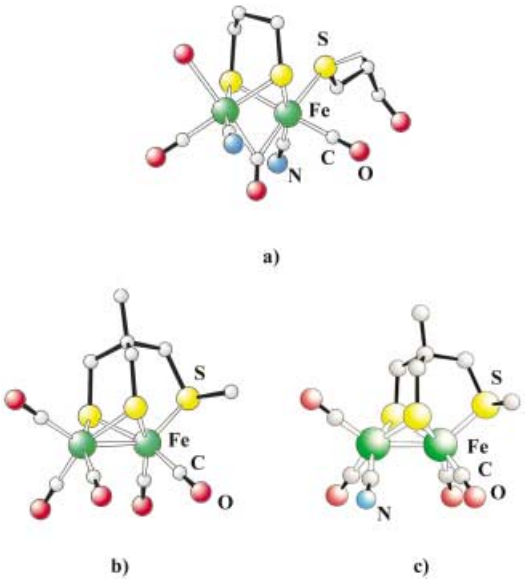

Figure 1. X-ray crystallographically determined structures of a) the di-iron subsite of the H centre of all-iron hydrogenase, this is a composite model combining features reported by Peters (PDB code 1FEH) and Nicolet (code 1HFE);[1, 2] b) the pentacarbonyl complex **A**;[7] c) monocyanide intermediate **C**.[12]

[a] Prof. C. J. Pickett, Dr. S. J. George, Z. Cui, M. Razavet
Department of Biological Chemistry, John Innes Centre
Norwich, NR4 7UH (UK)
Fax: (+44) 1603-450018
E-mail: chris.pickett@bbsrc.ac.uk

  0947-6539/02/0817-4037 $ 20.00+.50/0

which the bridging carbonyl has switched to a terminally bound mode with the re-formation of an Fe–Fe bond and the dissociation of the thioether ligand. Recent transient stopped-flow (SF) and spectroelectrochemistry data indicate that one-electron oxidation of **E** leads to an unstable Fe^{I}–Fe^{II} species with a bridging CO ligand and $\tilde{\nu}$(CO) frequencies near those observed in the CO-inhibited form of the oxidised H centre, thereby implying a role for this biologically unprecedented mixed-valence state in the natural system.[8]

Cyanation of carbonyl precursors is a key step in the synthesis of analogues of the subsite. Defining the mechanistic details of such reactions might give both information for the design of new functional materials[10] and an understanding of the biosynthesis of the subsite. In one of two independent studies of the cyanation reactions of {2Fe2S} systems, the monocyanide $[Fe_2(CO)_5\{CH_2(CH_2S)_2\}(CN)]^-$ was proposed as a direct intermediate on the pathway to the dicyanide $[Fe_2(CO)_4\{CH_2(CH_2S)_2\}(CN)_2]^{2-}$ from the hexacarbonyl $[Fe_2(CO)_6\{CH_2(CH_2S)_2\}]$,[9] whereas in the other study it was suggested that this is not the case.[10, 11] Both studies invoke bridging-CO transition states to explain the substitution chemistry.

This paper addresses the kinetics and intimate mechanisms associated with the pathway by which the {2Fe3S} – carbonyl **A** is converted to the {2Fe3S} dicyanide **D** and thence to the rearranged {2Fe2S} product **E**. It illustrates the role of bridging carbonyls in the assembly of the dicyanide species, how on – off sulfur ligation can have a dramatic effect on cyanation kinetics and how the {2Fe3S} core stabilises bridging carbonyl species.

Results and Discussion

The dicyanation of the {2Fe3S} assembly **A** to give the stable product **E** resolves into four well-defined steps involving three successively formed intermediates **B**, **C** and **D**, which have been spectroscopically characterised and their structures assigned, Figure 2. Under forcing conditions of high $[CN^-]$, the direct conversion of **B** to **E** can also occur. We have

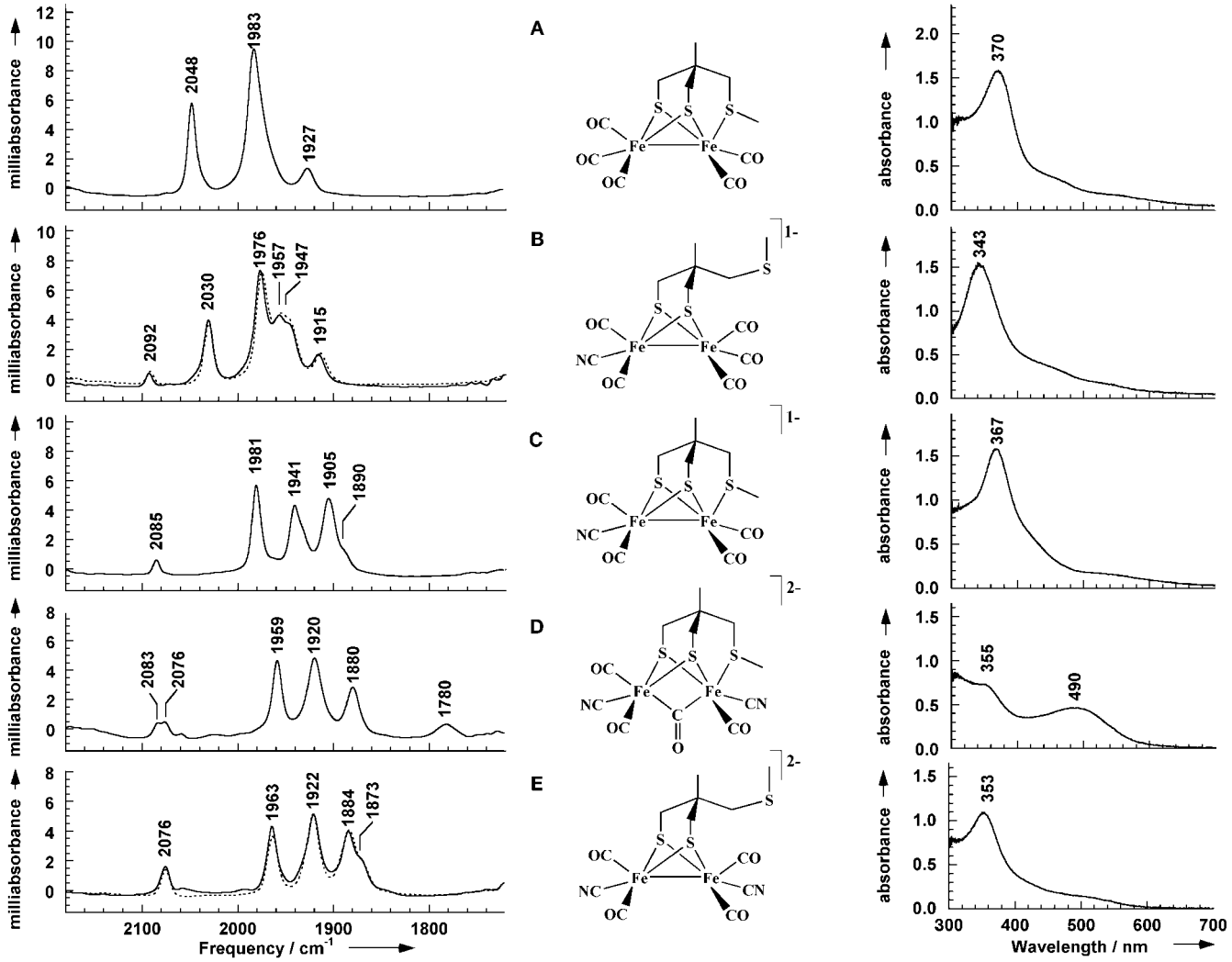

Figure 2. Infrared (left) and UV-visible (right) spectra of species **A** to **E** together with proposed structures (centre). Superimposed and normalised on the infrared spectra of **B** and **E** are corresponding data from the {2Fe2S} complexes $[Fe_2(CO)_5\{CH_2(CH_2S)_2\}(CN)]^-$ and $[Fe_2(CO)_4\{CH_2(CH_2S)_2\}(CN)_2]^{2-}$, respectively. The infrared spectra are normalised to a concentration of 0.58 mM. The optical spectra were obtained from a 0.18 mM complex.

0947-6539/02/0817-4038 $ 20.00+.50/0 *Chem. Eur. J.* **2002**, *8*, No. 17

identified a stable bridging carbonyl species and show that bridging-carbonyl transition states provide the key to understanding the overall substitution mechanism. In addition, we show that the primary substitution chemistry of the di-iron system involves an unprecedented on – off neighbouring-group participation of the tethered thioether ligand; this controls the reaction kinetics. That it also defines the stereochemistry of mono-cyanation is unambiguously established by X-ray structural analysis of the isolated monocyanide intermediate.[12]

The dicyanation pathway is summarised in Scheme 1. The experimental evidence supporting each of the four sequential steps I – IV in this Scheme is now given together with that for the high-[CN^-] pathway V from species **B** to species **E**. This is followed by a discussion of how optimal orientation of the facial ligands at the iron centres is sensitive to the arrangement of the propane dithiolate backbone substituents, and how this influences reaction rate. Finally, we discuss infrared and UV-visible characteristics of the species **A** – **E** and note an intense visible absorption that might provide a useful diagnostic for the formation or loss of a bridging CO in the enzyme or model systems.

Step I: Monocyanation with concerted thioether dissociation: The first step is the rapid binding of CN^- and displacement of the tethered methyl thioether from the iron atom to produce a monocyanide intermediate $[Fe_2\{MeSCH_2C(Me)(CH_2S)_2\}(CO)_5CN]^-$, **B** (Figure 2B).

The evidence for the nature of intermediate **B** is as follows. Firstly, titration experiments monitored by FTIR spectroscopy show stoichiometric binding of cyanide (data not shown). Secondly, the $\tilde{\nu}$(CO) and $\tilde{\nu}$(CN) region of the infrared spectrum of **B** is superimposable on that of the crystallographically defined {2Fe2S}-monocyanide complex $[Fe_2(S_2C_3H_6)(CO)_5CN]^-$, which has been independently characterised by Darensbourg[9] and Rauchfuss.[10] Thirdly, the UV-visible spectrum of **B** and that {2Fe2S}-monocyanide complex are dominated by the same absorption maxima at 343 nm (Figure 2B).[9] These observations are fully consistent with **B** and $[Fe_2(S_2C_3H_6)(CO)_5CN]^-$ possessing identical primary coordination spheres with any differential electronic effect caused by formal substitution at the remote 2-position of the propanedithiolate unit being, as expected, negligible.

The mechanism of the formation of **B** is revealed by analysis of the kinetic data obtained by SF-FTIR spectroscopy. The intermediate **B** is completely formed within a few seconds of adding a stoichiometric amount or small excess of $[Et_4N][CN]$ to **A**. The SF-FTIR data in Figure 3c show excellent isosbestic points, which reveal the clean formation of **B**. Typical time-course data are shown in Figure 3a. Under pseudo-first-order conditions, the rate shows a linear dependence on cyanide concentration, with a second-order rate constant of $1410\,M^{-1}s^{-1}$ (Figure 3b). This rate is independent of [CO] (Figure 3a).

The formation of the monocyanide with second-order reaction kinetics that are independent of [CO] clearly shows that the mechanism is associative (Scheme 2). We note that associative-substitution kinetics have previously been observed for the reaction of the related compounds $[Fe_2(CO)_6(SR)_2]$ ($R = CH_3$, CH_2CH_3, $CH_2C_6H_5$, C_6H_5, p-$C_6H_4CH_3$) with tertiary phosphines.[13] Darensbourg et al. have examined the kinetics of cyanide substitution on $[Fe_2(S_2C_3H_6)(CO)_6]$ and similarly invoke an associative pathway.[9] However, their reported substitution rate (21.5 °C) for this {2Fe2S} compound is about *10000-fold slower* than we observe with the {2Fe3S} complex. This dramatically underscores the role of the hemilabile thioether ligand in the substitution, as we discuss further below in the context of Scheme 2.

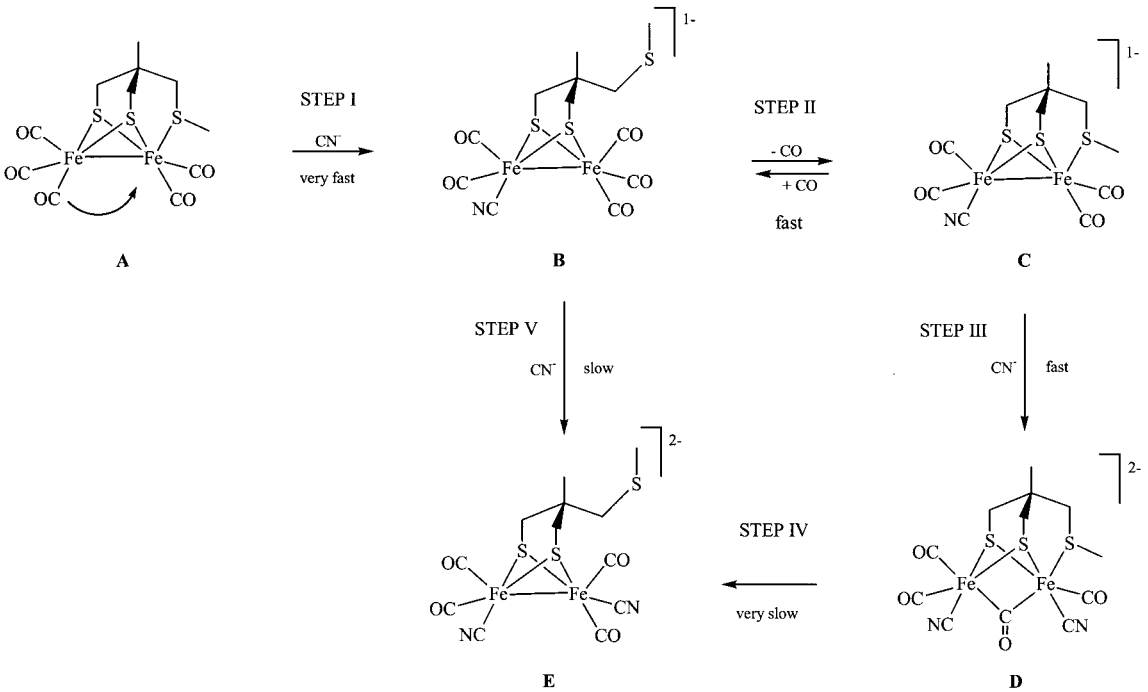

Scheme 1. Summary of the cyanation chemistry of **A**.

  0947-6539/02/0817-4039 $ 20.00+.50/0

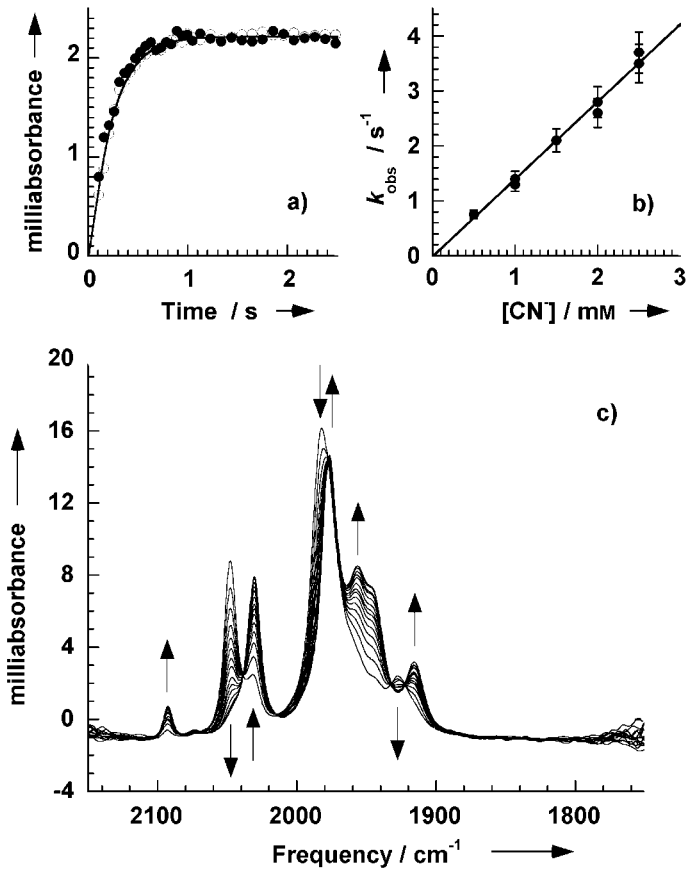

Figure 3. The monocyanation of **A** to **B** monitored by stopped-flow infrared spectroscopy. a) Example time course for the formation of **B** monitored at 2034 cm^{-1} in the absence (○) and presence (●) of CO. Initial [**A**] = 0.29 mM, [CN$^-$] = 2.5 mM. The line is a single-exponential fit. b) Cyanide dependence under pseudo first order conditions. Initial [**A**] = 0.055 mM. The solid line is for a cyanide dependent rate constant of 1410 M^{-1}s^{-1}. c) Example infrared spectra following the reaction. Initial [**A**] = 1.16 mM, [CN$^-$] = 2.5 mM.

Step II: Equilibrium rebinding of the thioether with CO displacement: In the absence of a significant excess of [Et_4N][CN], **B** loses CO to form **C**. The complex **C** has been isolated and characterised by X-ray crystallography (Figures 1c and 2C).[12] This unambiguously establishes the rebinding of the thioether with the loss of a CO ligand. The interconversion of **B** and **C** is fully reversible. The FTIR spectra show good isosbestic points (Figure 4a) and analyses of the time course data (Figure 4b) show that the rate *and* extent of formation of **C** is dependent on [CO]. The equilibrium constant for the reaction is estimated to be $K_d = 1.6$ mM with $k_{forward} = 0.6 \times 10^{-3}$ s^{-1} and $k_{back} = 0.39$ M^{-1}s^{-1} (Scheme 1).

The crystallographic structure of **C** shows that the cyanide ligand occupies the Fe site *distal* to the thioether ligated iron atom (Figure 1c). A solution FTIR spectrum obtained from a freshly redissolved crystal of **C** was identical with that in Figure 2C. The FTIR kinetics of subsequent steps (see below) show no evidence for isomeric interconversion in which cyanide is exchanged between the differentiated iron sites. These observations indicate that the initial attack of cyanide on **A** to give **B** occurs *exclusively* at the iron atom that is ligated by the three CO ligands rather than the thioether-ligated iron atom. Electronically, this is not surprising because the electron-donating nature of the thioether group would be expected to deactivate the metal to which it is attached with respect to associative attack. That the initial associative reaction to form **B** (Step I) is at least four orders of magnitude faster than substitution of {2Fe2S}-carbonyls, together with the regiospecificity of this reaction, is explained as follows. Attack on **A** by cyanide at the electron-poor $Fe(CO)_3$ centre takes place with the concerted formation of the bridged CO transition state **TS**, Scheme 2. Subsequent rapid but reversible dissociation of the thioether leads to the product **B** (or slower CO loss to the product **C**). The thioether ligand thus both

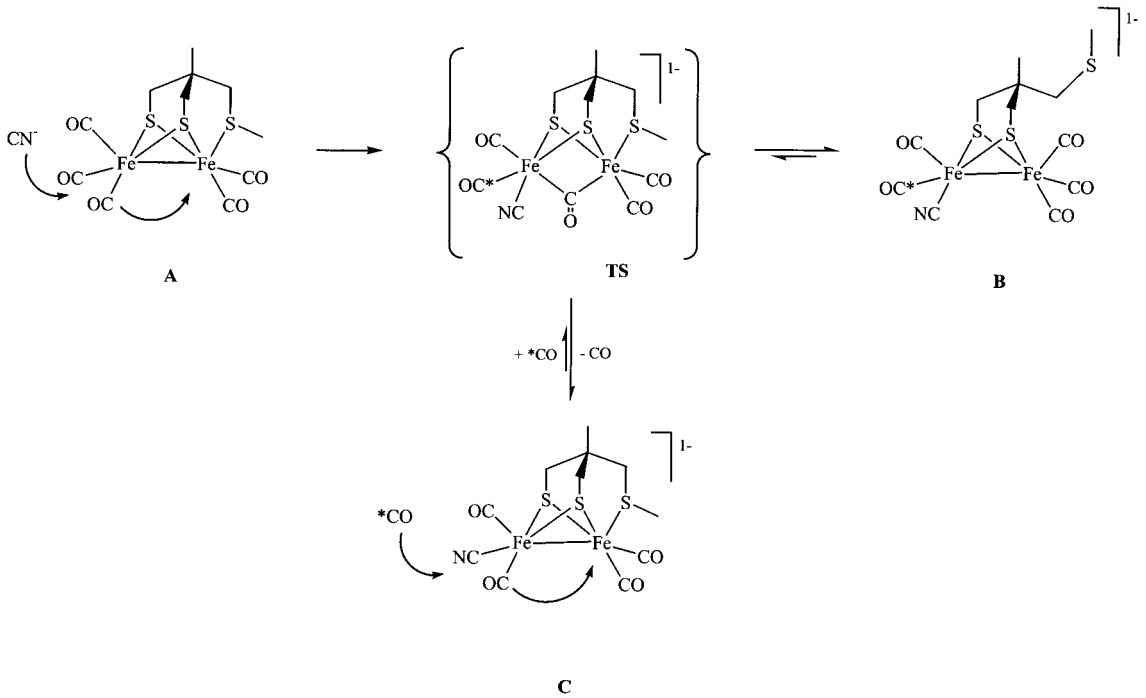

Scheme 2. The proposed role of a bridged CO monocyanide transition state **TS** in the reaction of **A** with cyanide to form **B** and the equilibrium of **B** and **C**.

0947-6539/02/0817-4040 $ 20.00+.50/0 *Chem. Eur. J.* **2002**, *8*, No. 17

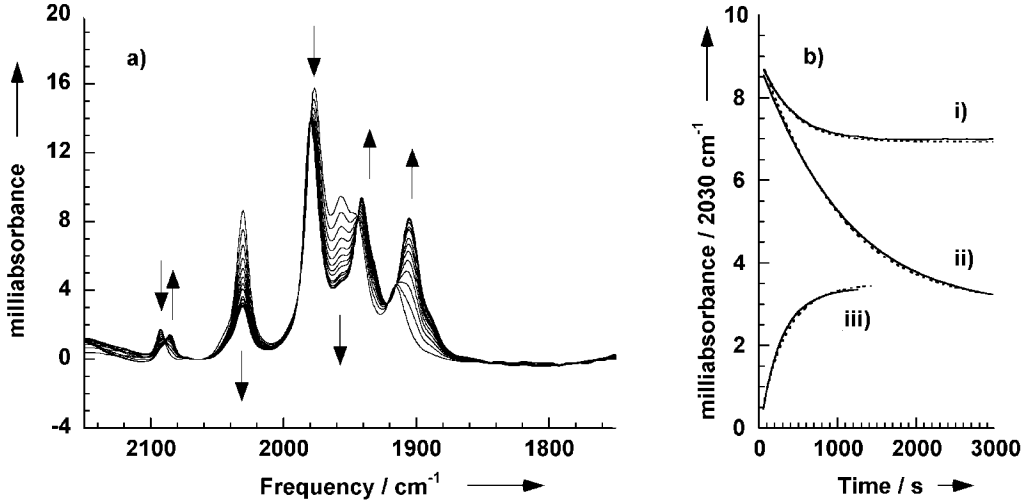

Figure 4. The equilibrium of **B** and **C** monitored by stopped-flow infrared spectroscopy. a) Example infrared spectra following the equilibration of 1.16 mM **B** in the absence of CO. b) Time courses (——) and numerical simulations (- - - -) i) Initial [**B**] = 1.16 mM, [CO] = 4.8 mM; ii) Initial [**B**] = 1.16 mM, no CO; iii) Initial [**C**] = 0.58 mM, [CO] = 6.4 mM. Experiments with "**B**" were in fact with **A** treated with a slight excess of CN^- (final concentrations 1.16 mM and 1.75 mM); this formed **B** within 3 s. **C** was similarly prepared in a closed bottled that was left for 3 h. The numerical simulations used $k_1 = 0.006\ s^{-1}$, $k_{-1} = 0.39\ M^{-1}s^{-1}$ and $K_d = 1.55$ mM.

stabilises the bridging-CO **TS** and functions as a good leaving group to provide a low-activation-energy pathway for substitution. In the {2Fe2S} system, the electron-withdrawing CO group is less effective in both of these roles, and the substitution kinetics are consequently much slower.

The reversibility of the conversion of **B** and **C** provides an opportunity to examine the regiospecificity of CO rebinding to **C**. Figure 5 compares the FTIR spectrum of unlabelled **B** with that of singly isotopically labelled **B** by using data taken

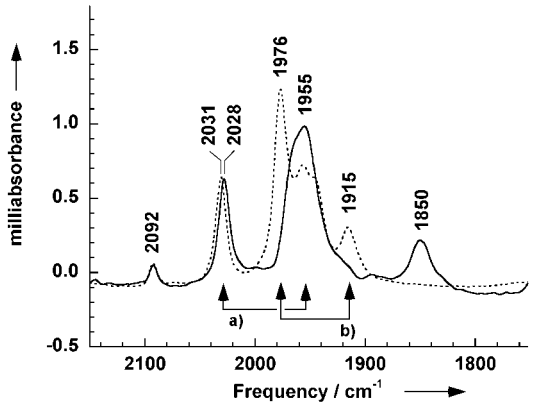

Figure 5. Infrared spectrum of **B** singly isotopically labelled with $^{13}C^{18}O$ (——) compared with unlabeled **B** (- - - -) obtained from stopped-flow infrared spectroscopy. The two spectra are normalised at the 2031/2028 cm^{-1} band. Compound **C** (0.58 mM) was incubated with $^{13}C^{18}O$ for less than one half-life (600 s, 34% conversion). The spectrum of unconverted **C** has been subtracted to give the figure. Spectra essentially identical in form were obtained at times at least up to 1200 s. Indicated are a) the isotopically invariant peaks and b) the isotopically sensitive bands of **B**.

600 seconds after adding $^{13}C^{18}O$ to **C**. The reaction was only 34% complete at this time. Two major bands at 2031 and 1957 cm^{-1} are essentially unaffected by the isotopic substitution. However, the bands at 1976 and 1915 cm^{-1} are completely lost and are replaced by an increase in intensity in the region of 1955 cm^{-1} and a band at 1850 cm^{-1}. This can be interpreted in terms of single isotopic substitution breaking vibrational coupling between two carbonyls with similar uncoupled $\tilde{\nu}$(CO) frequencies. Substitution for $^{13}C^{18}O$ should shift $\tilde{\nu}$(CO) frequencies by 91 cm^{-1}, so the new intensity at 1955 cm^{-1} arises from uncoupled $^{12}C^{16}O$, while the new band at 1850 cm^{-1} is $\tilde{\nu}(^{13}C^{18}O)$, the corresponding $\tilde{\nu}(^{12}C^{16}O)$ being 1941 cm^{-1}. We assign the isotopically invariant higher-energy pair to the $\{Fe(CO)_3\}$ site of **B** and the isotopically sensitive lower-energy bands to the more electron-rich $\{Fe(CO)_2(CN)\}$ site. Thus, the observations are readily rationalised by the labelled CO molecule attacking the cyanide-ligated iron atom, concerted migration of an unlabelled CO ligand and concomitant dissociation of thioether from the other iron (Scheme 2). The spectroscopic consequences of this are i) breaking the vibrational coupling of CO at the cyanide-ligated Fe atom to reveal uncoupled $\tilde{\nu}$ ($^{13}C^{18}O$) at 1850 cm^{-1} and $\tilde{\nu}$ ($^{12}C^{16}O$) near 1955 cm^{-1}, ii) leaving the higher-frequency modes at 2031 and 1957 cm^{-1} little changed. This CO-ligation pathway mirrors the initial cyanide attack on **A**, as both mechanisms proceed via the bridging-CO transition state **TS** with the site of attack on the iron centre distal to the thioether ligand. That formation of a bridging CO is intimately associated with the substitution chemistry at {2Fe3S} centres is spectroscopically demonstrated in the second cyanation step.

Step III: Dicyanation with formation of the metastable bridging carbonyl D: The reaction of **C** with a moderate excess of cyanide leads to the clean and complete formation of the species **D**. The SF-FTIR spectra show excellent isosbestic points with the growth of a bridging CO band at 1780 cm^{-1} (Figure 6c). Two $\tilde{\nu}$(CN) stretches at 2083 and 2076 cm^{-1} show that the two iron sites have differential ligation, and this has been confirmed by Mössbauer spectroscopy.[12] The data are consistent with **D**'s possessing the structure shown in Figure 2, in which the thioether remains coordinated to an iron atom following attack by cyanide.[7]

  0947-6539/02/0817-4041 $ 20.00+.50/0

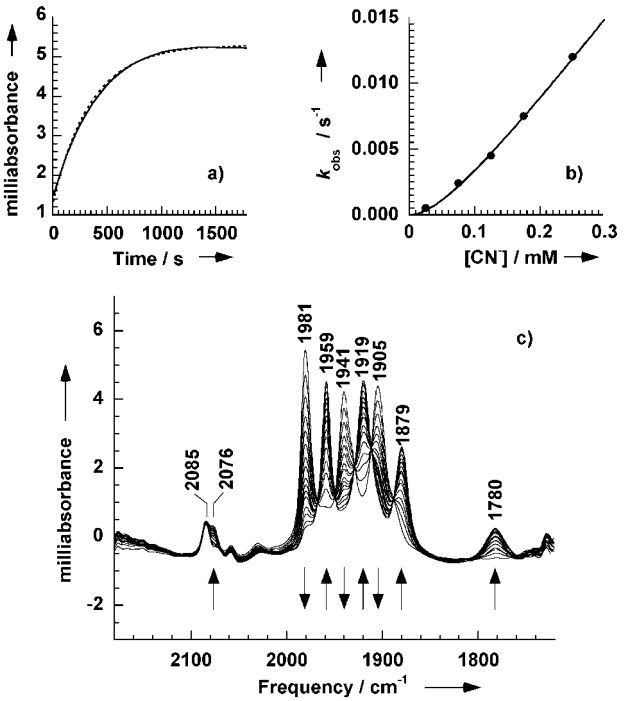

Figure 6. The reaction of **C** with cyanide to form **D** monitored by stopped-flow infrared spectroscopy. All samples have initial [**C**] = 0.58 mM. a) Example time course for the formation of **D** monitored at 1959 cm^{-1} (——) together with a single-exponential fit giving 2.4×10^{-3} s^{-1} (- - - -), [CN$^-$] = 75 mM. b) Cyanide dependence under pseudo first order conditions. Initial [**C**] = 0.58 mM. The line is a fit to Brønsted's equation (see text). c) Example infrared spectra following the reaction with 75 mM CN$^-$.

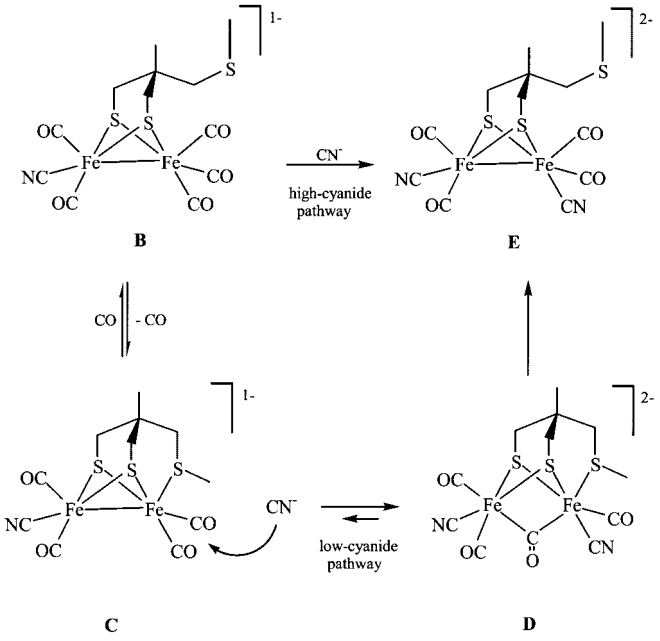

Scheme 3. The reactions of **B** and **C** with cyanide.

Figure 6a shows a typical time-course for the conversion of **C** to **D** under pseudo-first-order conditions with a single-exponential fit to the data. Figure 6b shows the dependence of the observed reaction rate k_{obs} on [CN$^-$]. The nonlinear plot is a consequence of the primary-kinetic-salt effect, in which for a anion – anion reaction $k_{apparent}$ must increase with the ionic strength of the media. The experimental curve can be fitted to Brønsted's equation[15] with a first-order dependence on cyanide concentration Figure 6b). This fit gives a second-order rate constant at zero ionic strength of 0.020 M^{-1} s^{-1} for the second cyanation step. The first-order dependence on cyanide is consistent with an associative attack of cyanide on the thioether-ligated Fe atom with the concerted shift of a terminal CO ligand into a bridging mode and the breaking of the metal – metal bond, conserving the stable 18-electron configuration about the iron atoms. As with the primary cyanation step I (Scheme 1), the incoming nucleophile attacks the more electron-poor iron centre (Scheme 3).

A clear difference in the chemistries of the {2Fe2S} and {2Fe3S} systems is that the latter supports the stabilisation of the bridging CO unit. This is rationalised by the thioether donor ligand compensating for the strongly withdrawing "keto" carbonyl group. In the {2Fe2S} system, charge withdrawn by any bridging-CO transition state must labilise *trans*-terminal carbonyls by diminishing back donation, thereby triggering metal – metal bond formation and the switching of the bridging CO into terminal-CO bonding mode: neither two cyanide ligands nor one cyanide and a thioether (cf. **C**) are alone sufficient to stabilise the CO bridge.

Step IV: {2Fe3S} – {2Fe2S} core rearrangement of D to give E: FTIR spectroscopy shows that **D** slowly rearranges at 25 °C to the thermodynamically stable final product **E** in which the bridging carbonyl has switched to a terminally bound mode with the re-formation of a Fe–Fe bond and the dissociation of the thioether ligand (Figure 2E, Scheme 3). Compound **E** is unequivocally the dicyanide with the thioether dissociated: the carbonyl/cyanide region of its infrared spectrum can be superimposed over that of the crystallographically defined complex $[Fe_2(CO)_4\{CH_2(CH_2S)_2\}(CN)_2]^{2-}$.[9, 10] We have followed this reaction by UV-visible spectroscopy, Figure 7b, and the kinetics fit to a single exponential with a rate constant of 6.5×10^{-5} s^{-1}. We note that the formation of the monocyanide complex **B** by the analogous rearrangement the bridged transition state **TS** (Scheme 2) must proceed at a rate which is at least *six orders of magnitude* faster than the conversion of **D** to **E**. This further underlines the need for an electron-donating cyanide ligand on *both* iron atoms to stabilise the bridging carbonyl group.

Step V: Dicyanation by attack of cyanide on the "{2Fe2S}" species B: The reaction of **B** with cyanide to give **E** directly takes place at a significant rate only under forcing conditions. For example, a 30-fold excess of cyanide (25 mM), generates **D** relatively cleanly via the formation of **C** (Figure 8a) with less than 13% of **E** formed via Step V. Thus under these conditions there is minimal attack on the "{2Fe2S}" core of **B** in a reaction analogous to that observed for the "simple" monocyanide $[Fe_2(CO)_5\{CH_2(CH_2S)_2\}(CN)]^-$. However, under the forcing conditions of a 300-fold excess of cyanide (250 mM), *direct* attack of cyanide on **B** to give **E** becomes a significant pathway that competes with the formation of **D** via **C** (Figure 8c, Scheme 3). This is a consequence of the [CN$^-$]-independent conversion of **B** to **C** becoming rate limiting. Numerical simulation with the three experimentally deter-

0947-6539/02/0817-4042 $ 20.00+.50/0 *Chem. Eur. J.* **2002**, *8*, No. 17

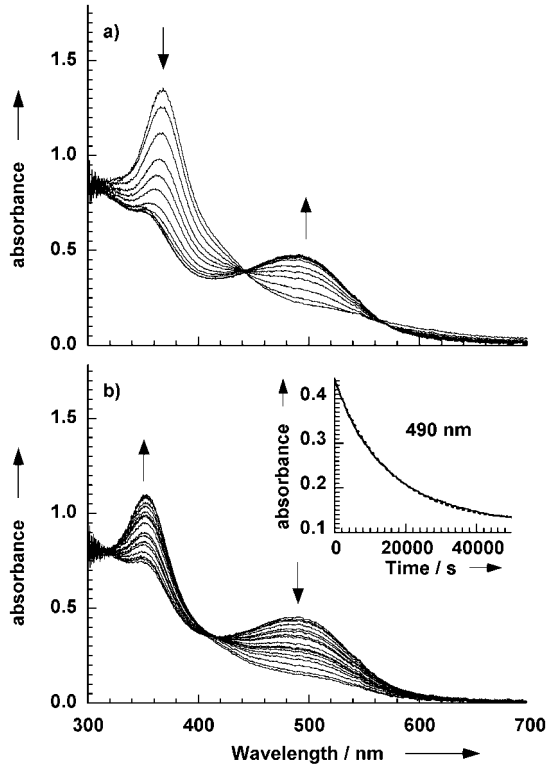

Figure 7. The reaction of a) **C** with cyanide to form **D** and b) the subsequent rearrangement of **D** to give **E** monitored by UV-visible spectroscopy. The insert is the time course measured at 490 nm (——) and single-exponential fit giving $6.5 \times 10^{-5}\,s^{-1}$ (----) for the loss of **D**. Initial [**C**] = 0.18 mM, [CN^-] = 50 mM.

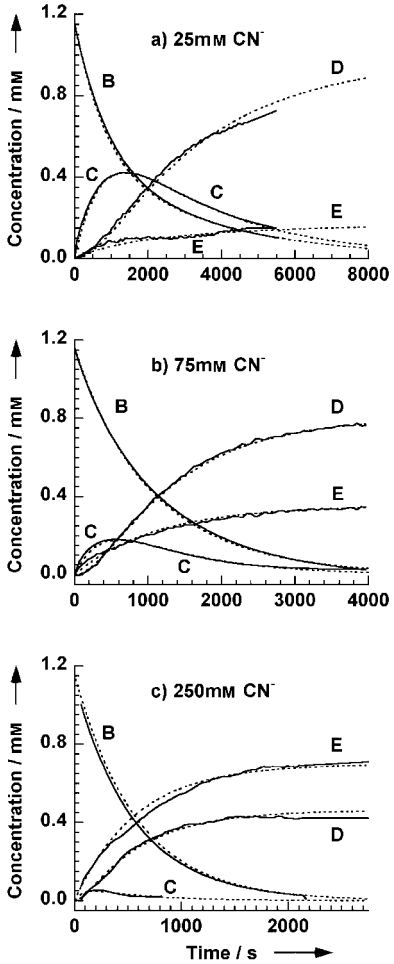

Figure 8. Time courses (——) and numerical simulations (----) for the reaction of **B** with cyanide monitored by stopped-flow infrared spectroscopy. a) 25 mM [CN^-], b) 75 mM [CN^-], c) 250 mM [CN^-]. The time courses have been normalised to concentration units. [**B**] was determined at 2031 cm^{-1}, [**C**] from the common crossover of **A**, **D** and **E** at 1934 cm^{-1}, [**D**] from the intensity of the 1780 cm^{-1} band and [**E**] at 1875 cm^{-1} corrected for the contribution of **D**. The rate constants used in the simulations for the direct reaction of **B** with cyanide to give **E** were: a) $3.5 \times 10^{-3}\,M^{-1}s^{-1}$, b) $3.8 \times 10^{-3}\,M^{-1}s^{-1}$, c) $4.2 \times 10^{-3}\,M^{-1}s^{-1}$.

mined rate constants for Steps II and III (IV is insignificant on this timescale) provides an estimate for the second-order rate constant of $0.004\,M^{-1}s^{-1}$ for step V (Figure 8). This kinetic analysis shows that **D** is not directly produced from **B**.[16] We discuss the stereochemical effects that determine the relative rates of cyanation of the {2Fe3S} and {2Fe2S} systems below.

Electronic and steric consequences of the pendant thioether on reaction rates: In the regioselective cyanation of **A** to give **B**, the thioether locks the conformation of the {Fe-$(CO)_2$(SMe)} unit, but leaves the {$Fe(CO)_3$} free to rotate. Darensbourg et al. have suggested that a staggered conformation, as shown in Scheme 4, may be a required precursor to the formation of a carbonyl bridge in {2Fe2S} systems, and that such a conformation is readily accessed and not energetically limiting at ambient temperatures.[9] In the case of the {2Fe3S} system **A**, cyanide can attack with concerted formation of a bridged-CO low-energy transition state that is stabilised by the predisposed *trans*-thioether group provided by the locked conformation (Scheme 4). This stereoelectronic effect may also contribute to the extraordinary rate enhancement of this monocyanation over that of [$Fe_2(CO)_6${CH_2-$(CH_2S)_2$}].[9]

The complex [$Fe_2(CO)_5${$CH_2(CH_2S)_2$}$(CN)]^-$ has FTIR and UV/vis spectroscopic features essentially indistinguishable from **B**. Therefore, with respect to the primary coordination sphere, the two species can be considered as "electronically identical". However, the rate constant for the direct attack of cyanide on **B** is almost forty times smaller than the $0.146\,M^{-1}s^{-1}$ reported for its attack on [$Fe_2(CO)_5${CH_2-$(CH_2S)_2$}$(CN)]^-$.[9] The explanation for this difference most likely resides with steric factors, and can be rationalised by the propane dithiolate substituents preventing adoption of the optimum geometry for either cyanide attack in one conformer or bridge formation in the other (Scheme 4). Notably, Rauchfuss and co-workers have provide crystallographic evidence for the close approach of a methyl bridgehead substituent to a carbonyl in related *N*-methylazapropane dithiolate complexes.[6]

The rate constant for the attack of cyanide on **C** is about five-fold greater than it is for attack on **B**, despite the expected deactivation of the iron atom towards nucleophilic attack by the electron-donating thioether ligand. Given that the attacked iron centre in **B** is sterically encumbered, as it is in the locked geometry of **C**, the difference in rate constants might rest with the thioether ligand stabilising a product-like

  0947-6539/02/0817-4043 $ 20.00+.50/0

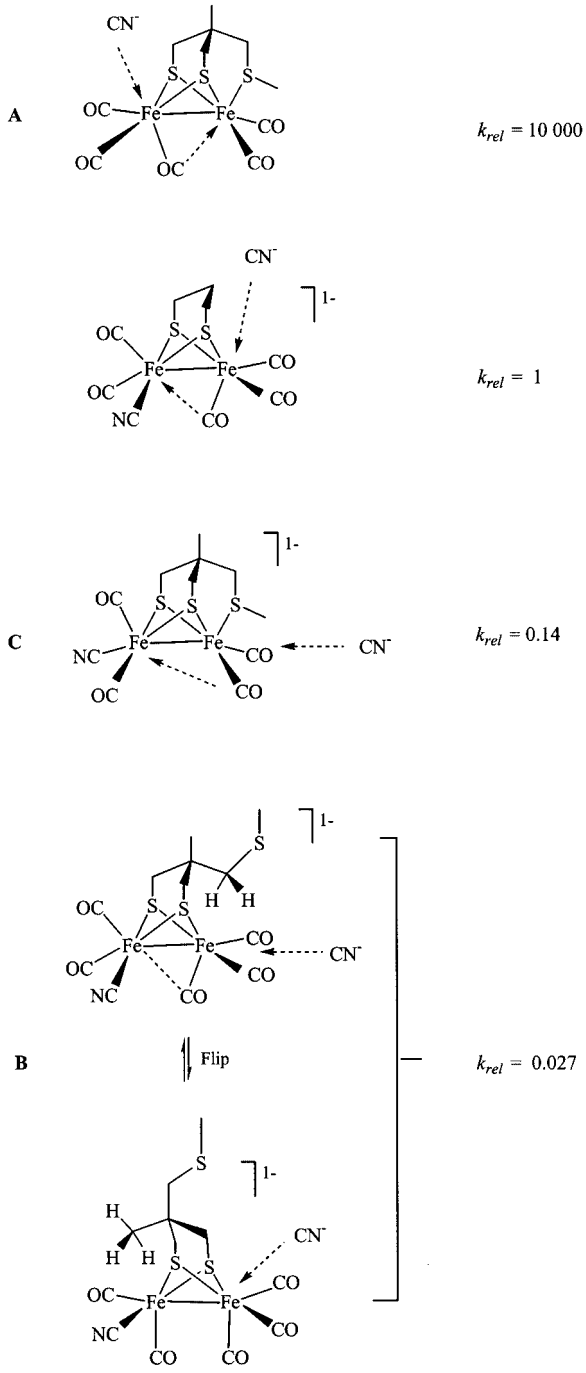

Scheme 4. Steric factors influencing the cyanation of **A**, **C** and **B**. The rates are relative to that for the {2Fe2S} complex $[Fe_2(CO)_5\{CH_2(CH_2S)_2\}(CN)]^-$: 0.146 $M^{-1}s^{-1}$.

transition state as a CO approaches a bridging mode and this more than compensating for its deactivating electron-donor nature.

Comparative FTIR and UV-visible spectroscopic data for species A – E: Figure 2 shows FTIR and corresponding UV-visible spectra for the species **A** – **E**. There is a striking similarity in the patterns of the FTIR spectra of **C** and **E**, species that are formally related by the replacement of the ligating SMe group by CN^-. The bands in **C** are all shifted to a lower frequency by approximately 20 cm^{-1} on conversion to **E**. This relatively small shift observed on replacing the neutral thioether ligand by anionic cyanide attests to the strong donating ability of the SMe group. That all the bands shift by approximately the same amount suggests that the ligand charge is delocalised across both iron atoms. Species **D**, which possesses both two cyanide ligands and a ligated SMe, has three terminal $\tilde{\nu}$(CO) modes close to those of **E**. This implies that the bridging CO group is strongly electron-withdrawing, an effect which is compensated for by the bound SMe ligand.

Figure 2 shows the optical data for the complexes **A** – **E**. The spectra for metal – metal bonded species **A**, **B**, **C** and **E** all show a dominant absorption in the UV at or below 370 nm with broad weaker features at lower energies, as do the spectra of the {2Fe2S} systems reported by Darensbourg.[9] The major electronic transition shifts to the red on formal replacement of CO by cyanide. For example, in $[Fe_2(CO)_6\{CH_2(CH_2S)_2\}]$, the band is at 327 nm, in the monocyanides $[Fe_2(CO)_5\{CH_2(CH_2S)_2\}(CN)]^-$ and **B** it is at 343 nm, whilst in $[Fe_2(CO)_4\{CH_2(CH_2S)_2\}(CN)_2]^{2-}$ and **E** it occurs at 353 nm. Formal substitution of CO in $[Fe_2(CO)_6\{CH_2(CH_2S)_2\}]$ by an SMe as in **A** also results in a red shift from 327 to 370 nm. The intramolecular substitution of CO in **B** by SMe to form **C** results in a smaller red shift from 343 to 367 nm. Clearly electron-donating groups at the {2Fe2S} core decrease the energy separation between the donor and acceptor orbitals involved in the transition but do not seem to significantly modify the electronic manifold. This is in stark contrast to the consequence of introducing a bridging CO ligand. The electronic spectrum of **D** is dominated by a new broad band in the visible region at 490 nm which has peak width at half height of 80 nm. There is only a weak transition in the UV region at 355 nm. Such a dramatic change indicates significant alteration in electronic structure. The dominant charge-transfer band in the spectrum of $[Fe_2(CO)_6(S_2)]$ is observed at 335 nm with a weak shoulder at 425 nm and these have been assigned to transitions from the "bent" Fe–Fe bond comprising the HOMO (a_1) to its antibonding counterpart, which comprises the LUMO (b_2), and from "lone-pair" Fe(3d) orbitals.[17] The UV transitions observed for the metal – metal bonded species **A**, **B**, **C** and **E** are undoubtedly analogous, and it is most likely that the visible transition observed for **D** involves charge transfer from Fe (3d) to the bridging C=O π^*.

The loss of absorption intensity around 350 nm and the appearance of a low energy band, signalling the loss of an Fe–Fe bond and formation of a CO bridge (cf. Figure 7a), might thus be a useful diagnostic in kinetic and spectroscopic studies of the enzyme system.

Conclusion

Here we summarise the principal conclusions of this study of the cyanation of a {2Fe3S} system.

i) Stepwise substitution chemistry: There are four successive steps with three isolatable intermediates in the dicyanation reaction of the {2Fe3S} – carbonyl. Each step was studied in

0947-6539/02/0817-4044 $ 20.00+.50/0 *Chem. Eur. J.* **2002**, *8*, No. 17

isolation; this allowed a full spectroscopic and kinetic dissection of the whole reaction pathway.

ii) On – off role of tethered thioether group: The ability of the tethered thioether group to dissociate upon the initial attack by cyanide on the {2Fe3S} core has dynamic and steric consequences. Firstly, there is an over 10^4-fold increase in the rate of monocyanation of **A** vis-à-vis the {2Fe2S} system reported by Darensbourg et al.[9] Secondly, the monocyanide product **B** is formed regioselectively, the cyanide binds at the Fe atom distal to that from which the thioether dissociates. Thirdly, rebinding of thioether to the monocyanide reversibly eliminates CO to form **C**. Fourthly, attack of a second cyanide molecule takes place on the thioether-ligated monocyanide **C** about five times faster than on the CO-ligated/SMe-dissociated intermediate **B** and gives a bridging CO intermediate **D**. Finally, **D** rearranges to the thermodynamically stable product **E** by dissociation of the thioether, conversion of the bridging CO to a terminal mode and regeneration of a metal – metal bond.

iii) The role of bridging CO in substitution at di-iron centres: The regiospecific formation of the monocyanide **B** and the isotopically detected regioselective regeneration of **B** from thioether-ligated **C** provide experimental support for the involvement of bridging-CO transition states in the substitution chemistry of the di-iron assemblies. This is underlined by the direct spectroscopic characterisation of the bridged-CO intermediate **D**.

iv) Stabilisation of bridging CO: The attack of CN^- on **C** gives the bridged-CO intermediate **D**, whereas attack on **B** does not give a spectroscopically detectable CO-bridged species. The presence of a thioether ligand and the dianionic charge introduced by dicyanation appear to be the key factors in stabilising the bridge. We estimate that the bridge-to-terminal-CO conversion takes place at least 10^6 times faster for the monoanionic **TS** than for **D**. In the dicyanide, the electron-donating ability of the thioether prevents labilisation of a CO ligand *trans* to the strongly electron-withdrawing "keto" carbonyl bridge. Recent work has shown that oxidation of **E** generates a transient {2Fe3S} cyanide core with bridging CO and a Fe^{I}–Fe^{II} mixed-valence state[8] attesting to the ability of an {2Fe3S} core to stabilise a bridging CO configuration in a higher oxidation state, as is observed in the CO-inhibited enzyme system.[1–3]

v) Observation of a potentially diagnostic electronic transition in the visible region: The Fe^{I}–Fe^{I} metal – metal-bonded systems are characterised by a sharp absorption band in the UV region around 350 nm. The breaking of this bond during the formation of a bridging carbonyl is signalled by the appearance of a low energy band in the visible region at 490 nm. This might thus be a useful diagnostic probe in fast kinetic studies seeking to identify short-lived CO-bridged transients in model chemistry and possibly in turnover studies of the enzyme system.

vi) Comments on {2Fe3S} systems and the natural subsite/H cluster: The distal Fe atom of the subsite of all-iron hydrogenase possesses a labile water molecule that can be replaced by inhibitory CO.[2] It has been reasonably postulated that it is at this distal Fe atom that a proton is bound, reduced to hydride and thence evolved as dihydrogen following protic attack—a process mediated by an azapropane bridge functioning as a proton-transfer intermediary.[3, 4] However, there is little explicit in this model that would explain the need for a binuclear rather than mononuclear subsite neither that invokes the need for bridging CO in turnover states. We note that in our model {2Fe3S} system, bridging CO is strongly electron-withdrawing, as evidenced by comparison of the terminal stretching frequencies of **D** and **E** (Figure 2B and D). Thus an electron-withdrawing bridging CO ligand *trans* to ligated H_2O at the distal iron of the subunit should substantially enhance the acidity of the bound water and thence the possibility of a prototrophic shift to the proximal iron, possibly by conformational flipping of the azapropane bridge (Scheme 5).

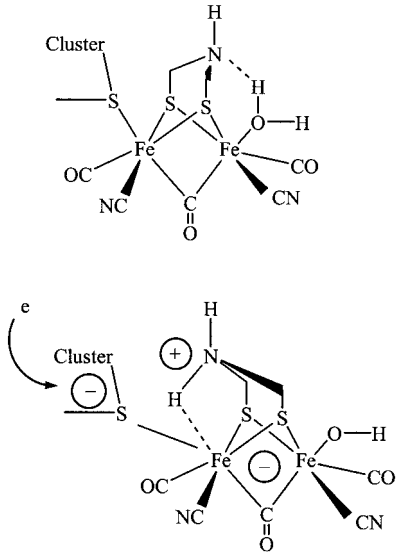

Scheme 5. *Possible* role of the bridging CO in a prototrophic shift at the di-iron subsite.

Finally, the step-wise dicyanation of the synthetic {2Fe3S} system is controlled through dissociation/association of the pendant thioether group. It is not inconceivable that the cysteinyl S group bridging the subsite to the {4Fe4S} cluster might possibly function in a similar fashion during H-centre biosynthesis or even during turnover of the enzyme.

Experimental Section

Stopped-flow FTIR spectroscopy: Stopped-flow FTIR (SF-FTIR) experiments were performed by using an adapted Bruker IFS 66/S spectrometer (Bruker UK Ltd., Coventry, UK) fitted with a liquid-nitrogen-cooled mercury cadmium telluride (MCT) detector. The stopped-flow circuit and cell were home-built and described elsewhere.[14, 18, 19] The drive system and stopped-flow cell were entirely housed within an anaerobic dry glove box (< 1 ppm O_2) (Belle Technology, Portesham, Dorset, UK).[19] The sample cell temperature was maintained at 25 °C for all experiments by means of a

water-cooled jacket. The cell path length was calibrated to 48.2 μm. For these experiments the instrument collected data between 2200 and 1700 cm^{-1}. Typically, for an infrared resolution of 4 cm^{-1}, the time resolution was 25 ms per spectrum, and the dead-time before detection was 18 ms. Exact sample conditions are given in the Figure legends.

Analyses of time-dependent spectra, as well as fitting and numerical simulation of time-courses were all carried out by using home-written software. The simulation programs employed the RKSUITE suite of subroutines, which are an implementation of the Runge – Kutta method.[20]

UV-visible spectroscopy: UV-visible measurements were performed entirely within the same anaerobic glove box used for the SF-FTIR measurements with an Ocean Optics SD 2000 fibre-optic spectrophotometer (Ocean Optics Inc, Florida, USA) and a TOPS Mini-D2 light source (Avantes, Eerbeek, The Netherlands). The optical cell had a path length of 10 mm. With this configuration a good quality, 2 nm resolution, optical spectrum can be collected at least once every second.

Sample preparation: The complex $[Fe_2(CO)_5\{MeSCH_2C(Me)(CH_2S)_2\}]$ was prepared as previously described.[7] $[Et_4N][CN]$ (Aldrich) was dried at 80 °C under vacuum. Acetonitrile was distilled over CaH_2 prior to use. All manipulations were usually performed in a glove box (< 1 ppm O_2) under dinitrogen and occasionally by Schlenk techniques. Solutions for stopped-flow infrared and time-resolved UV/visible spectroscopies were prepared immediately before use and kept in the dark.[21] CO solutions were quantitated by the IR band of free CO at 2128 cm^{-1} by using CO-saturated acetonitrile as a standard.[22] All concentrations for stopped-flow experiments are quoted after mixing.

Acknowledgements

We thank the BBSRC and the John Innes Foundation for supporting this work.

[1] Y. Nicolet, C. Piras, P. Legrand, C. E. Hatchikian, J. C. Fontecilla-Camps, *Structure* **1999**, *7*, 13 – 23.
[2] J. W. Peters, W. N. Lanzilotta, B. J. Lemon, L. C. Seefeldt, *Science* **1998**, *282*, 1853 – 1858.
[3] a) A. J. Pierik, M. Hulstein, W. R. Hagen, S. P. J. Albracht, *Eur. J. Biochem.* **1998**, *258*, 572 – 578; b) A. L. de Lacey, C. Stadler, C. Cavazza, E. C. Hatchikian, V. M. Fernandez *J. Am. Chem. Soc.* **2000**, *122*, 11 232 – 11 233; c) Y. Nicolet, A. L. de Lacey, X. Vernede, V. M. Fernandez, E. C. Hatchikian, J. C. Fontecilla-Camps, *J. Am. Chem. Soc.* **2001**, *123*, 1596 – 1601.
[4] Y. Nicolet, B. J. Lemon, J. C. Fontecilla-Camps, J. W. Peters, *Trends Biochem. Sci.* **2000**, *25*, 138 – 143.
[5] a) E. J. Lyon, I. P. Georgakaki, J. H. Reibenspies, M. Y. Darensbourg, *Angew. Chem.* **1999**, *111*, 3373 – 3376; Angew. *Chem. Int. Ed.* **1999**, *38*, 3178 – 3180; b) M. Schmidt, S. M. Contakes, T. B. Rauchfuss, *J. Am. Chem. Soc.* **1999**, *121*, 9736 – 9737; c) A. Le Cloirec, S. P. Best, S. J. Borg, S. C. Davies, D. J. Evans, D. L. Hughes, C. J. Pickett, *Chem. Commun.* **1999**, 2285 – 2286.
[6] a) J. D. Lawrence, H. X. Li, T. B. Rauchfuss, M. Bernard, M. M. Rohmer, *Angew. Chem.* **2001**, *113*, 1818 – 1821; *Angew. Chem. Int. Ed.* **2001**, *40*, 1768 – 1771; b) H. X. Li, T. B. Rauchfuss, *J. Am. Chem. Soc.* **2002**, *124*, 726 – 727.
[7] M. Razavet, S. C. Davies, D. L. Hughes, C J Pickett, *Chem. Commun.* **2001**, 847 – 848.
[8] M. Razavet, S. J. Borg, S. J. George, S. P. Best, S. A. Fairhurst, C. J. Pickett, *Chem. Commun.* **2002**, 700 – 701.
[9] E. J. Lyon, I. P. Georgakaki, J. H. Reibenspies, M. Y. Darensbourg, *J. Am. Chem. Soc.* **2001**, *123*, 3268 – 3278.
[10] F. Gloaguen, J. D.Lawrence, M. Schmidt, S. R. Wilson, T. B. Rauchfuss, *J. Am. Chem. Soc.* **2001**, *123*, 12 518 – 12 527.
[11] Our preliminary data on this compound, taken at 25 °C, show that $[Fe_2(CO)_6\{CH_2(CH_2S)_2\}(CN)]^-$ is a detectable intermediate on the pathway to the dicyanide product.
[12] M. Razavet, S. C. Davies, D. L. Hughes, E. J. Barclay, D. J. Evans, C. J. Pickett, unpublished results.
[13] P. C. Ellgen, J. N. Gerlach, *Inorg. Chem.* **1973**, *12*, 2526 – 2532.
[14] S. J. George, G. A. Ashby, C. W. Wharton, R. N. F. Thorneley, *J. Am. Chem. Soc.*, **1997**, *119*, 6450 – 6451.
[15] I. N. Levine, *Physical Chemistry*, McGraw Hill, New York, **1978**.
[16] At high cyanide concentrations, a band at 1844 cm^{-1} formed at long times. This band was not kinetically associated with any other observed infrared feature. We assign it to a minority species possibly arising from further cyanation and CO loss. Importantly, we did not observe any analogous evidence for cluster damage in the other steps, **I** – **IV**.
[17] B. K. Teo, M. B. Hall, R. F. Fenske, L. F. Dahl, *Inorg. Chem.* **1975**, *14*, 3103 – 3117.
[18] A. J. White, K. D. Drabble, C. W. Wharton, *Biochem. J.* **1995**, *306*, 843 – 849.
[19] R. N. F. Thorneley, S. J. George in *Prokaryotic Nitrogen Fixation: A Model System for Analysis of a Biological Process* (Ed.: E. W. Triplett), Horizon Scientific Press, Wymondham, UK, **2000**, pp. 81 – 100.
[20] Softreport 92-S1, Department of Mathematics, Southern Methodist University, Dallas, TX, USA, **1992**.
[21] We have found that the cyanation chemistry of the {2Fe2S} complex $[Fe_2(CO)_6\{CH_2(CH_2S)_2\}]$ can be significantly affected by photolysis from ambient light, hence all experiments on the {2Fe3S} complex were performed in the dark.
[22] The saturating concentration of CO in acetonitrile was determined to be 13.4 mm by titrating microlitre quantities of the solution into aqueous horse-heart myoglobin (0.5 mL).

Received: April 16, 2002 [F4023]

  0947-6539/02/0817-4046 $ 20.00+.50/0